available at www.sciencedirect.com

SCIENCE DIRECT®

journal homepage: www.elsevier.com/locate/biochempharm

Differential processing of antitumour-active and antitumour-inactive *trans* platinum compounds by SKOV-3 ovarian cancer cells

Angelina Boccarelli [a], *Domenico Giordano* [a], *Giovanni Natile* [b], *Mauro Coluccia* [a,*]

[a] *Department Biomedical Sciences and Human Oncology, University of Bari, Piazza Giulio Cesare 11, 70124 Bari, Italy*
[b] *Department Pharmaceutical Chemistry, University of Bari, via Orabona 4, 70125 Bari, Italy*

ARTICLE INFO

Article history:
Received 15 December 2005
Accepted 18 April 2006

Keywords:
Platinum anticancer drugs
Trans geometry
Iminoether, SKOV-3 tumour cells
Cell-cycle
Gene expression

ABSTRACT

In order to compare the mechanistic properties of the antitumour-active *trans* platinum complex *trans*-[$PtCl_2${*Z*-HN = C(OMe)Me}(NH_3)] (*trans*-*Z*) and of the antitumour-inactive isomer of cisplatin *trans*-[$PtCl_2(NH_3)_2$] (*trans*-DDP), the differential processing of the two compounds by SKOV-3 ovarian cancer cells has been investigated. *trans*-Z and *trans*-DDP enter cells with the same efficacy, but *trans*-Z shows a two-fold higher affinity for cellular DNA. The treatment with *trans*-DDP IC_{50} determines an initial and transient cytostatic effect, paralleled by a moderate increase of apoptosis and by sequential and reversible arrests in S and G_2/M phases of cell-cycle. In contrast, *trans*-*Z* IC_{50} determines an initial cytotoxic effect, a more persistent and marked increase of apoptosis, and a more marked and prolonged arrest in S and G_2/M phases of the cell-cycle. Treatment-induced gene expression modifications indicate that phenotypic effects of *trans*-DDP are driven by an initial and transient up-regulation of some genes related to cell-cycle checkpoint and arrest networks, whereas the more dramatic phenotypic effects of *trans*-*Z* are driven by a persistent up-regulation of more numerous genes involved in cell-cycle checkpoint and arrest networks, and in genome stability and DNA repair. Therefore, molecular and cellular events have been identified which are produced by *trans*-*Z* but not by *trans*-DDP, and which likely represent the mechanistic basis of antitumour activity of *trans*-*Z* in the SKOV-3 system.

1. Introduction

Cisplatin (*cis*-diamminedichloroplatinum(II), *cis*-DDP) is one of the most largely used DNA-damaging agents in cancer chemotherapy, but its clinical efficacy is limited by intrinsic or acquired resistance as well as by significant side effects [1]. Therefore, much attention has focused on designing new platinum complexes with a broader range of antitumour activity and/or improved pharmacological properties. Most of them are characterized by *cis* geometry because the *trans*-isomer of cisplatin (*trans*-diamminedichloroplatinum(II), *trans*-DDP or transplatin) is inactive. It is generally accepted that transplatin inactivity depends upon two major factors: (i) kinetic instability and consequent susceptibility to deactivation, and (ii) DNA interaction regioselectivity and structural perturbations different from those of cisplatin [2]. However, several exceptions to the general rule that two leaving groups in *cis* position are necessary for antitumour activity of platinum complexes, have been reported. Among such complexes are those with N-donor aromatic etherocycles, iminoethers, cyclohexylamine, and ramified aliphatic amines [3]. Substitution of more bulky ligands for ammines in

* *Corresponding author*. Tel.: +39 080 5478 412; fax: +39 080 5478 524.
E-mail address: mauro.coluccia@dimo.uniba.it (M. Coluccia).
0006-2952/$ – see front matter
doi:10.1016/j.bcp.2006.04.021

trans-DDP has produced compounds with higher in vitro tumour cell growth inhibitory potency, often active towards cisplatin-resistant tumours, and in some cases also endowed with significant in vivo activity. From a mechanistic point of view, the bulky ligands can retard substitution reactions of the two chloride ions, thus reducing the kinetic instability of transplatin. On the other hand, DNA adducts formed by antitumour-active *trans* platinum complexes are qualitatively and quantitatively different from those of cisplatin, indicating that cisplatin-like DNA adducts are not obligatory determinants for antitumour activity of platinum compounds.

The platinum complex with two iminoether ligands *trans*-[$PtCl_2${*E*-HN = C(OMe)Me}$_2$] has been the first example of *trans* platinum species showing in vivo antitumour activity [4,5], and the main pharmacological properties of this class of complexes as well as of other antitumour-active *trans* platinum complexes have been recently reviewed [6]. Briefly, the platinum–iminoether complexes, whose tumour cell growth inhibitory effect depends upon DNA adduct formation, are characterized by having: (a) in vitro tumour cell growth inhibitory potency higher than that of *trans*-DDP, along with the ability of overcoming cisplatin resistance associated to decreased accumulation and glutathione detoxification, (b) significant in vivo antitumour activity towards leukemic and solid murine tumours [7–9], and (c) peculiar DNA binding mode, characterized by the formation of stable monofunctional adducts on purine residues [10–13]. It has also been demonstrated that the presence of only one iminoether is sufficient for obtaining the antitumour activation of the *trans* geometry, for instance the *trans*-[$PtCl_2(NH_3)${*Z*-HN = C(OMe)Me}] (*trans*-*Z*) complex shows an in vivo antitumour activity similar to that of cisplatin in murine p388 leukemia as well as in SKOV-3 human cancer xenografts [14]. Importantly, *trans*-*Z* has a spectrum of activity different from that of cisplatin, and is active towards cisplatin-resistant tumour cells [15]. In order to contribute to an understanding of the nature of DNA adducts potentially responsible of its pharmacological activity, DNA interaction properties of *trans*-*Z* have been carefully investigated in comparison to those of *trans*-DDP [14,15]. In the reaction with DNA fragments and/or selectively modified oligonucleotides, both *trans*-*Z* and *trans*-DDP form monofunctional adducts on guanine residues that slowly evolve into interstrand cross-links with the complementary cytosines. However, the rate of closure of *trans*-*Z* monofunctional adducts is about two times slower than that of corresponding *trans*-DDP monofunctional adducts. In addition, the *trans*-*Z* interstrand cross-link behaves as a hinge joint, increasing the flexibility of the double helix, whereas the *trans*-DDP interstrand cross-link behaves as a directed bend and introduces less flexibility into the helix [16].

With the aim of further investigating the mechanism of pharmacological action of *trans*-*Z*, cellular accumulation and DNA platination of SKOV-3 ovarian cancer cells have been investigated in this study. SKOV-3 cellular response to equitoxic concentrations of *trans*-*Z* or *trans*-DDP has also been analyzed in parallel as far as growth inhibition, cell-cycle modifications, and gene expression modifications are concerned. The results highlight previously unknown cellular and molecular determinants of the *trans*-*Z* pharmacological action, thus providing valuable clues for further development of antitumour platinum compounds with *trans* geometry.

2. Materials and methods

2.1. Tumour cells and platinum complexes

The SKOV-3 ovarian cancer cell line was obtained from the National Cancer Institute, Biological testing Branch (Frederick, MD, USA), and maintained in the logarithmic phase at 37 °C in 5% CO_2 humidified air in RPMI 1640 medium supplemented with 10% fetal calf serum, 2 mM glutamine, penicillin (100 U/ml), and streptomycin (0.1 mg/ml). *Trans*-[$PtCl_2(NH_3)${*Z*-HN = C(OMe)Me}] (*trans*-*Z*) was synthesized as already reported [14], while *trans*-[$PtCl_2(NH_3)_2$] (*trans*-DDP) was purchased from Sigma–Aldrich Chemie GmbH (Schnelldorf, Germany).

2.2. Cellular and DNA platination

The platinum complexes were added at different equimolar concentrations and for 3 h to approximately 3×10^6 tumour cells growing exponentially. Immediately after exposure, cell monolayers were washed three times with ice-cold phosphate-buffered saline (PBS), scraped, and harvested in 0.5 ml phosphate buffered saline (PBS). Samples, held on ice, were sonicated (Soniprep 150, Fisons, Loughborough, England). Total intracellular platinum content was determined by flameless atomic absorption spectroscopy (FAAS, Varian model SpectrAA 880 Zeeman). Cellular platinum levels were expressed as nmol platinum/mg protein, protein being determined from 50-μl aliquots using the Bio-rad protein determination kit (Bio-rad Laboratories, Italy).

For DNA platination measurements, different equimolar concentrations of platinum complexes were added for 3 h to approximately 8×10^7 SKOV-3 cells grown to near confluence in 175-cm^2 tissue culture flasks. After exposure, cell monolayers were washed three times with ice-cold PBS, and DNA was isolated from cell pellets according to standard procedures [17]. Briefly, the pellets were lysed using the extraction buffer (10 mM Tris, 100 mM EDTA, 20 μg/ml RNase, 0.5% sodium dodecyl sulphate, pH 8.0), treated with proteinase K (1 mg/ml) at 37 °C for 30 min and then at 50 °C for 2 h. DNA was isolated by phenol extraction and ethanol precipitation, and then hydrolysed in 0.2% nitric acid. The DNA content of the hydrolysate was determined by the Burton assay [18], with the nucleic acid base content determined by measuring the absorbance at 600 nm. The platinum content of the hydrolysate was measured by FAAS.

2.3. Octanol/saline partition ratios

Partition ratios of platinum complexes were determined in an *n*-octanol/saline system, as previously described [8]. Briefly, platinum complexes were dissolved and diluted to 50 μM in saline. A 1.5-ml aliquot of the solution was added to an equal volume of octanol in a glass tube and shaken mechanically for 15 min. Tubes were centrifuged (1500 rpm, 5 min) and aliquots carefully removed from the top octanol and the bottom aqueous layers for platinum determination by FAAS and octanol/saline partition ratios calculation.

2.4. Cell growth and death kinetics, and cell cycle progression modifications

Exponentially growing SKOV-3 cells were seeded in 10-cm^2 culture plates (80,000 cells/ml); after 24 h, cells were exposed to IC_{50} concentrations of *trans*-Z or *trans*-DDP (120 and 170 μM, respectively) over a 96 h continuous treatment [15]. At different time points (0, 12, 24, 48, 72, and 96 h), cell growth, cell cycle, and gene expression were evaluated in parallel. Viable cell count was performed on both adherent and non-adherent cells by the trypan blue exclusion test. For cell cycle analysis, adherent cells were washed, incubated with 0.2% trypsin for 5 min, and collected by centrifugation (1200 rpm, 10 min). Cell pellets were washed in PBS, and fixed in 1 ml ice-cold 70% ethanol. Fixed samples, containing 1×10^6 cells, were centrifuged, rinsed once in PBS, treated with 50 μg/ml RNase for 30 min at 37 °C, and then stained with 50 μg/ml propidium iodide (Sigma–Aldrich Chemie GmbH). A minimum of 20,000 cells were run on a Coulter Epics Profile II Flow cytometer (Beckman Coulter, IL SpA, Italy). Cell cycle distribution was performed by using the Multicycle software provided by Phoenix Flow Systems (San Diego, USA). For apoptosis determination, fragmented DNA was removed from non-adherent cells [19], therefore apoptotic cells were made visible as a peak below the G_1 DNA content, and quantitated using the ''overlapped peak'' multicycle fitting option.

2.5. RNA extraction, and gene expression assay

Total RNA was isolated from SKOV-3 cells at each time point (about 10 μg/sample) using TRIzol® reagent (Invitrogen, Italy) according to the manufacturer's instructions. RNA was quantified by UV spectroscopy, and its quality was determined by ethidium bromide staining after agarose/formaldehyde electrophoresis.

The expression profile of 188 genes known to be associated with maintaining genome stability and regulating cell-cycle progression was analyzed by using GEArrayTM Q series cDNA expression array membranes (SuperArray Inc., Bethesda, MD, USA). Total RNA (3.5 μg/assay) was used as template for [α^{32}P]cDNA probe synthesis ([α^{32}P]dCTP, Amersham; gene-specific primer mixture, SuperArray) by the MMLV-RT (Promega Italia, Milano) according to the manufacturer's instructions. cDNA probes were denatured and then hybridized overnight with the expression array membranes. The membranes contain gene fragments (about 500 bp) belonging to two major functionally-characterized groups: (i) genome stability/DNA repair and checkpoint genes, and (ii) cell-cycle genes (listed at http://www.superarray.com, GEArray Q Series, Human Genome Stability/DNA Repair Gene Array, and Human Cell-cycle Gene Array, SuperArray Inc., Bethesda, MD, USA), and specifically selected to minimize potential cross-reactivity with related genes. In the membrane format each gene is reproduced in quadruplicate, and controls (plasmid DNA, blanks, and house-keeping genes) are printed across the base of the membrane. After hybridization, the membranes were washed twice with 2× saline sodium citrate buffer (SSC)/1% sodium dodecyl sulphate (SDS), twice with 0.1× SSC/0.5% SDS, and then data were acquired with a phosphor screen scanner (Cyclone, and OptiQuant software, Packard Instruments). Data were exported to Microsoft Excel spreadsheets, and analysed (pUC 18 plasmid DNA background subtraction, and normalization to GAPDH house-keeping gene) by the GEArray Analyzer software (SuperArray Inc.). Each experiment was performed twice with similar results, the duplicate results for each gene being within 8% of the mean for that gene. The mean values of the two series are presented for the genes whose expression was at least 4% of that of GAPDH.

3. Results

3.1. Cellular and DNA platination

Fig. 1 shows total intracellular accumulation and DNA platination of *trans*-Z and *trans*-DDP in SKOV-3 cells after 3-h exposure to various concentrations of platinum complex. Platinum accumulation was linearly dependent upon drug concentration (Fig. 1a), and the cells retained their integrity (trypan blue exclusion) even at the higher dose explored (400 μM, not shown). Cellular accumulation of *trans*-Z was almost identical to that of *trans*-DDP. This result correlates

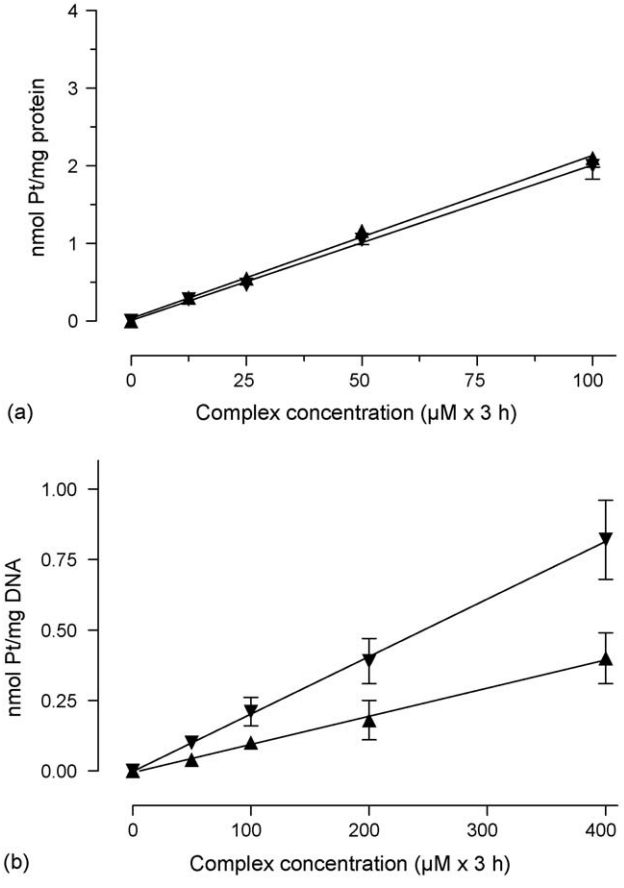

Fig. 1 – Intracellular platinum accumulation (a) and DNA platination (b) of SKOV-3 cells after a 3-h exposure to *trans*-DDP (▲) or *trans*-Z (▼) (points: means; bars: ± S.D.; *n*: two triplicate experiments). Lines were linear by regression analysis of the data points of the two complexes for both cellular accumulation and DNA platination (r^2 = 0.99).

with the similar *n*-octanol/saline partition ratios of the two complexes (0.27 and 0.30 for *trans*-Z and *trans*-DDP, respectively) which in turn indicate a similar lipophilicity. SKOV-3 DNA platination after 3-h exposure to 0–400 μM *trans*-Z or *trans*-DDP is shown in Fig. 1b. DNA adduct formation for *trans*-Z was about two-fold higher than that for *trans*-DDP, this revealing a major affinity of the platinum–iminoether complex for cellular DNA. From these results, total intracellular accumulation and DNA platination after 3-h exposure to IC_{50} concentrations of *trans*-Z and *trans*-DDP (120 and 170 μM, respectively) can be calculated. The intracellular accumulation of *trans*-DDP and *trans*-Z corresponds to 3.6 (95% CI = 3.3–3.9) and 2.4 (95% CI = 2.3–2.5) nmol Pt/mg protein, respectively, whereas DNA platination corresponds to 0.17 (95% CI = 0.16–0.19) and 0.23 (95% CI = 0.21–0.25) nmol Pt/mg DNA, respectively.

3.2. *Cell growth and death kinetics, and cell-cycle progression modifications*

To evaluate the effects of platinum complexes on tumour cell growth curve, exponentially growing SKOV-3 cells were exposed to *trans*-DDP or *trans*-Z IC_{50} over a period of 96 h. At different time intervals (0, 12, 24, 48, 72, and 96 h) the viability of adherent and non-adherent cells was measured by the trypan blue exclusion test. In parallel, the percentage of apoptosis among non-adherent cells was evaluated by measuring the amount of DNA fragmentation by flow cytometry. The number of adherent cells at each time interval is given as percentage of cell number at time 0 (Fig. 2a). After 96 h, the percentages were 140%, 130%, and 260% for the *trans*-DDP, *trans*-Z, and control, respectively. Although the number of adherent cells at the end of the treatment was comparable

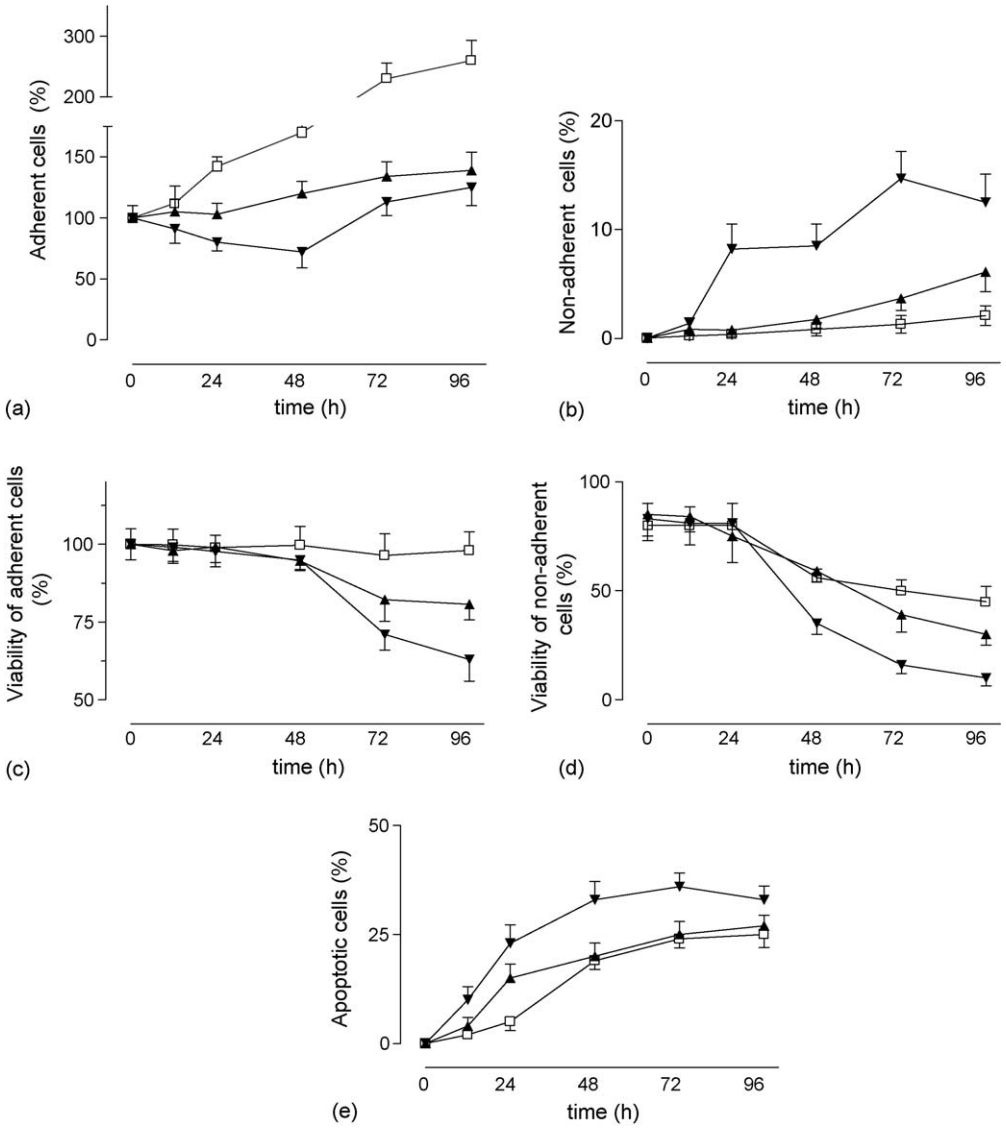

Fig. 2 – Cell growth and death of SKOV-3 cells during continuous exposure to *trans*-DDP (▲) or *trans*-Z (▼) IC_{50} concentrations (□, control). (a) Adherent cells remaining as a percentage of cell number at time zero, and (b) non-adherent cells as a percentage of total cell number at different time points. Percentage viability of adherent and non-adherent cells at different time points is shown in (c) and (d), respectively (trypan blue exclusion assay); (e) Percentage of apoptosis among non-adherent cells at different time points (fraction of total cells in the sub-G_1 peak on DNA frequency distribution histograms).

for the *trans*-DDP- and the *trans*-Z-treated samples, the time-course was rather different. In the case of *trans-Z*, adherent cells progressively decreased up to 48 h, then they increased to about 130% at 96 h. In contrast, in the case of *trans*-DDP, adherent cells did not show significant variations at 12 and 24 h, then they gradually increased reaching finally about the same level of *trans*-Z-treated cells.

The number of detached cells was calculated as a percentage of the total number of cells present at each time point (Fig. 2b). In parallel to the precocious reduction of adherent cells, *trans*-Z initiated cellular detachment at a faster rate than *trans*-DDP. At 24 and 48 h time intervals, approximately 8% of *trans*-Z-treated cells had detached, this percentage further increasing to about 13% at 72 and 96 h incubation times. In contrast, *trans*-DDP did not determine a significant increase of detached cells up to 48 h incubation time, and only about a 5% of detached cells was observed at 72 and 96 h. Cell viability was estimated by measuring the number of cells with intact plasma membranes by the trypan blue exclusion test. The percentage of viable adherent and non-adherent cells across the different time intervals is shown in Fig. 2c and d, respectively. The viability of both adherent and non-adherent cells did not show significant variations up to 24 h incubation with *trans*-Z or *trans*-DDP. In the following time intervals, the viability of adherent and non-adherent cells progressively decreased and reached at the end of the treatment (96 h) the values of 60% and 10% (for adherent and non-adherent cells, respectively), in the case of *trans*-Z and 80% and 30% in the case of *trans*-DDP.

To further investigate the type of cell death induced by platinum complexes, both adherent and non-adherent SKOV-3 cells were analyzed by flow cytometry staining to determine the hypodiploid DNA (fragmented DNA) percentage. In the case of adherent cells, the detection of apoptotic cells as sub-G_1 peak on DNA content frequency histograms gave a negative result (not shown), likely due to the relatively low cytotoxic effect of IC_{50}; in contrast, apoptotic cells were detected among non-adherent cells, and results are shown in Fig. 2e. *Trans*-Z increased the number of apoptotic cells, compared with control, in the time interval 12–72 h; then, the percentage of apoptotic cells decreased to values similar to control. In contrast, *trans*-DDP increased apoptotic cells only at 24 h time interval, the percentage of apoptotic cells being similar to control for all other time intervals.

Flow cytometric analysis of the effects of *trans*-Z or *trans*-DDP on the progression of SKOV-3 cells through the cell cycle is reported in Fig. 3. Exposure to *trans*-Z IC_{50} resulted initially (12 and 24 h) in a reduction of cell percentage in G_1-phase with a parallel increase of cell percentages in S and G_2/M phases. The G_2/M accumulation reached the maximum value after 48 h; then the G_2/M accumulation gradually decreased, while the G_1 percentage increased, so that by the end of the exposure the cell-cycle distribution of *trans*-Z-treated cells had approached that of control cells. Exposure to *trans*-DDP IC_{50} produced cell-cycle modifications qualitatively similar to those of *trans*-Z, i.e. an early reduction of G_1 percentage along with an increase of S- and G_2/M-phase cells (12 h), followed by a residual G_2/M accumulation at 24 h. However, cell-cycle modifications induced by *trans*-DDP were less marked and less persistent than those of *trans*-Z, and the cell cycle distribution approached more rapidly that of control cells.

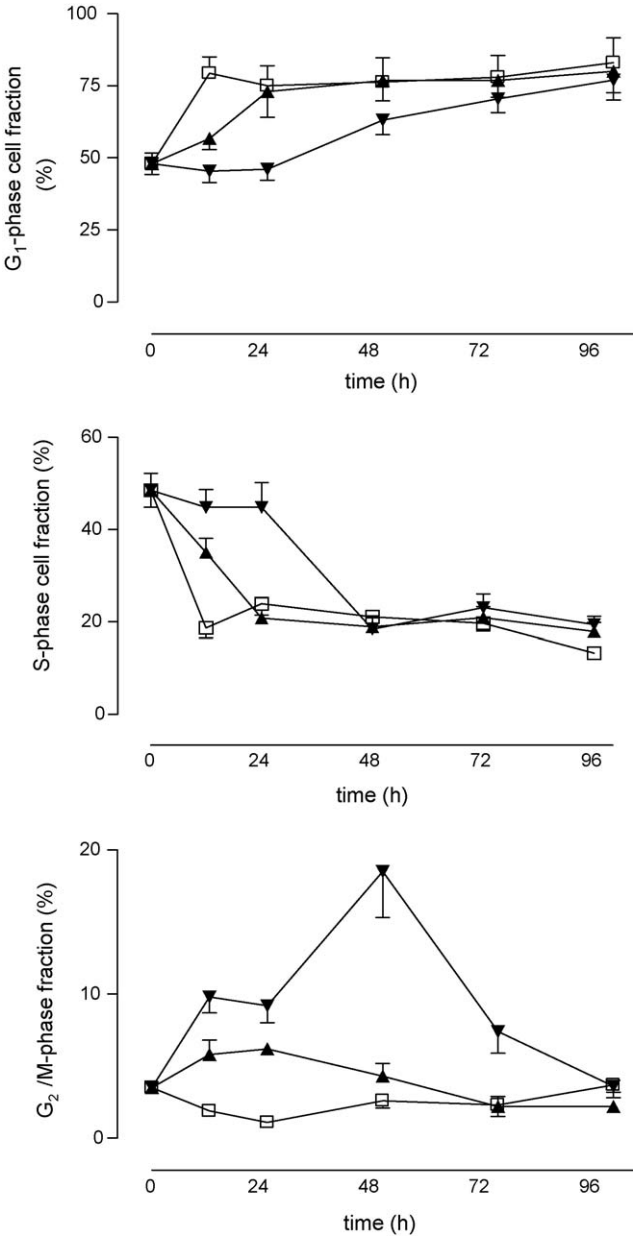

Fig. 3 – Percentages of SKOV-3 cells in G_1, S, and G_2/M phases of the cell cycle during continuous exposure to *trans*-DDP (▲) or *trans*-Z (▼) IC_{50} concentrations (□, control); points: means; bars: ±S.D.; *n*: two triplicate experiments.

3.3. *Pathway-specific gene expression modification*

The time-course of expression profile of 188 genes known to be associated with maintaining genome stability and regulating cell-cycle progression was analyzed by using GEArrayTM cDNA expression array membranes, in order to determine the treatment-induced modifications. The panel includes base excision repair, nucleotide excision repair, mismatch excision repair, double strand breaks repair, post-replicative repair, and cell-cycle progression regulatory genes. We started with this highly selected microchip for gene array instead of an all-encompassing gene array because the selected genes entail a

well-characterized profile governing genome stability and cell proliferation, hence simplify data acquisition, analysis and interpretation, and avoid rationalization of genes not functionally characterized.

Results relative to the genes whose expression in treated and/or control SKOV-3 cells was at least 4% of that of GAPDH house-keeping gene are shown in Fig. 4A–C, and also in Table 1. In the genome stability/DNA repair and checkpoint functional group, the expression pattern of APEX1, NEIL3, UNG, G22P1, DDB1, XRCC4, XRCC5, and UBE2V2 genes appeared uniform through the 96 h incubation time and was similar for treated and control cells (Fig. 4A). It can be concluded that SKOV-3 cells express in a rather uniform manner mRNAs for some endonucleases of base excision repair (APEX1, NEIL3, UNG), damage-specific DNA binding protein-1 (DDB-1) of nucleotide excision repair, p70 and p80 components of Ku protein (G22P1, XRCC5), XRCC4 protein of double strand break repair, and ubiquitin-conjugating enzyme UBE2V2.

The genome stability/DNA repair and checkpoint genes whose expression was modified by *trans*-DDP or *trans*-Z, are summarized in Fig. 4B. In the case of *trans*-DDP, 12 h after the beginning of treatment the level of expression of the growth arrest and DNA-damage-inducible α gene (GADD45A, 21% of GAPD) increased by more than two times with respect to control, the gene remaining up-regulated also at 24 h. At 48 h, the expression of the telomeric repeat binding factor 2 (TERF2, 100% of GAPD), ubiquitin protein ligase E3A (UBE3A, 20% of GAPD), ubiquitin-activating enzyme E1 (UBE1, 13.5% of GAPD), and SMT3 suppressor (SUMO1, 11.5% of GAPD) genes increased by about three times. Finally, at 72 h the expression of DNA-activated protein kinase gene (PRKDC, 22% of GAPD) increased by about three times.

In the case of *trans*-Z-treated SKOV-3 cells, 12 h after the beginning of the treatment, several genes were induced to levels 2–3 times higher than control. They include ubiquin C (UBC, 58% of GAPD), growth arrest and DNA-damage-inducible, α (GADD45A, 24% of GAPD), RAD23 homolog A (RAD23A, 18% of GADP), ubiquitin protein ligase E3A (UBE3A, 13% of GAPD), and RAD18 homolog (RAD18, 11% of GAPD) genes. SKOV-3 cells maintained the up-regulation of RAD23A, UBE3A, and RAD18 up to 72 h, and of UBC and GADD45A up to 96 h. A second group of genes became up-regulated (by a factor of 2–3) after 24 h and generally maintained this condition up to 72 h.

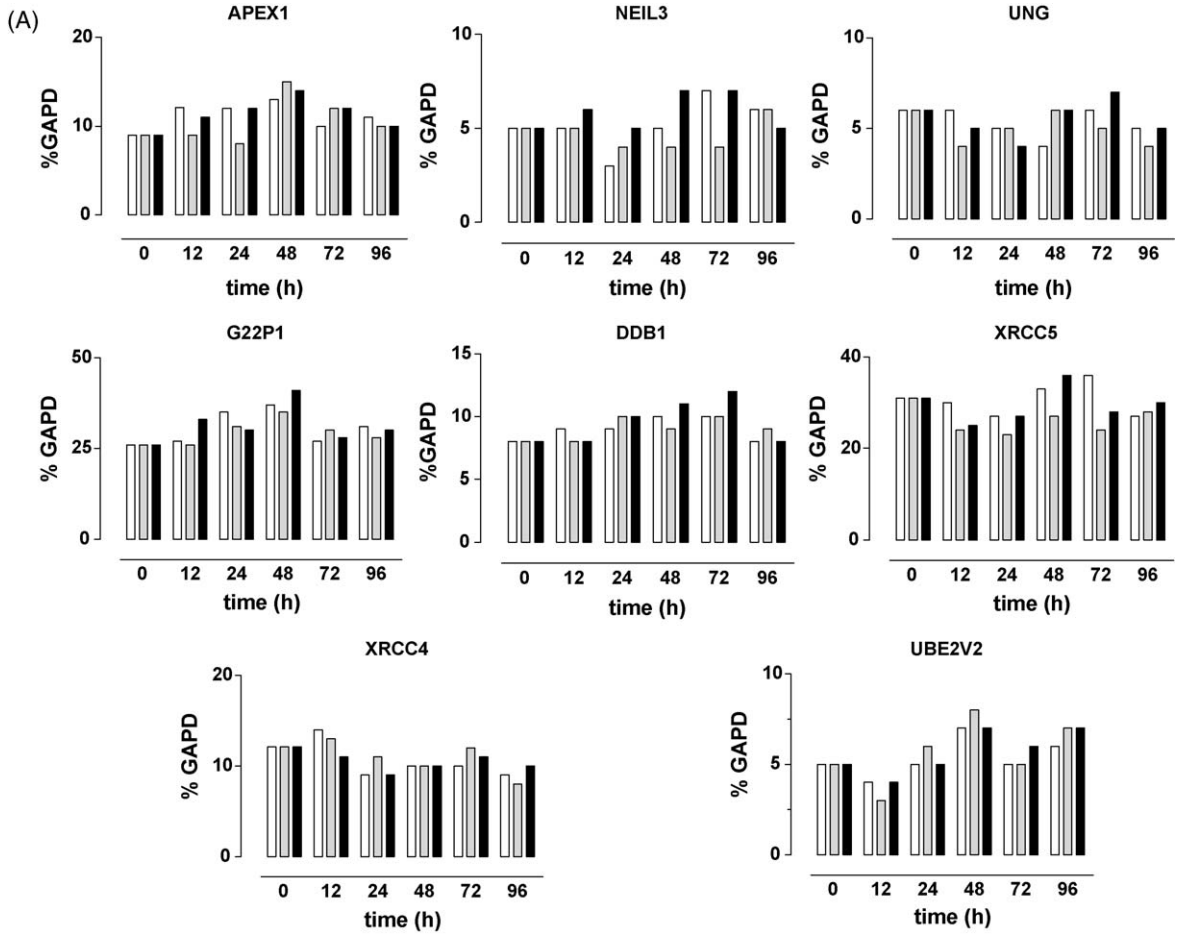

Fig. 4 – Time-course analysis of the pathway-specific gene expression of SKOV-3 cells exposed to *trans*-DDP or *trans*-Z IC_{50}. (A, B) The figures summarize the expression profile of 117 genome stability/DNA repair and checkpoint genes whose expression was not modified (A) or modified by the treatment (B). (C) The figure summarizes the expression profile of 71 genes related to cell-cycle progression. Only results for genes whose expression was detectable are shown, as percentage of GAPDH housekeeping gene (white bars, control; grey bars, *trans*-DDP; black bars, *trans*-Z).

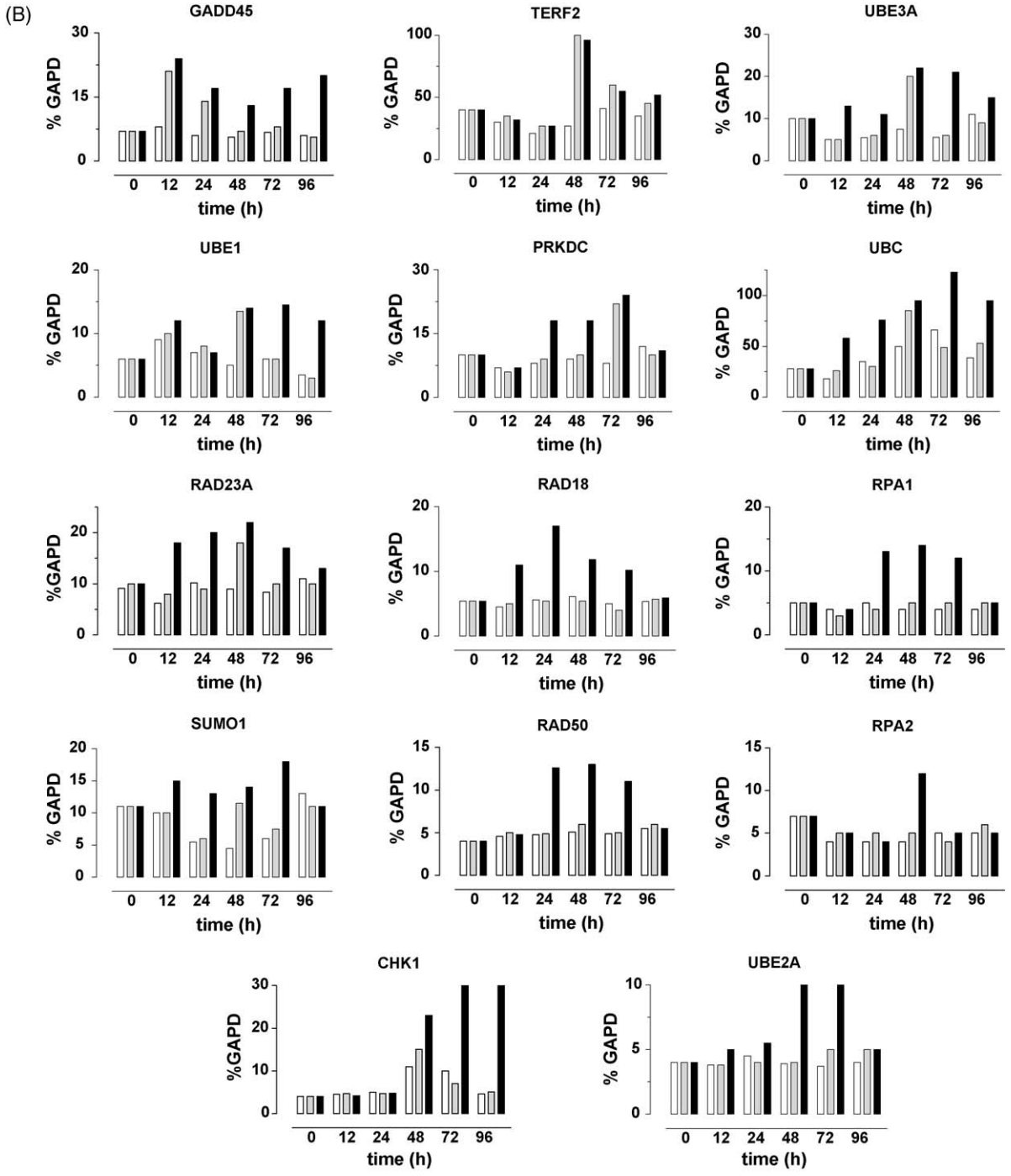

Fig. 4. (Continued)

They include: DNA-activated protein kinase (PRKDC, 18% of GAPD), replication protein A1 (RPA1, 13% of GAPD), SMT3 suppressor (SUMO1, 13% of GAPD), and RAD50 homolog (RAD50, 12% of GAPD). A third group of genes became up-regulated by a factor of 2–3 only after 48 h. They include telomeric repeat binding factor 2 (TERF2, 96% of GAPD), CHK1 checkpoint homolog (CHK1, 23% of GAPD), ubiquitin-activating enzyme E1 (UBE1, 14% of GAPD), Replication protein A2 (RPA2, 12% of GAPD), and ubiquitin-conjugating enzyme E2A (UBE2A, 12% of GAPD). The up-regulation of TERF2 decreased gradually at 72 and 96 h; RPA2 receded to control levels at 72 h, whereas UBE2A maintained the overexpression up to 72 h, and CHK1 and UBE1 up to 96 h.

The expression of genes involved in cell-cycle progression is shown in Fig. 4C. The gene expression of control cells had mostly a bell-shaped pattern, with highest values around 48–72 h. Transplatin-treated cells had an expression pattern similar to that of control cells, with the exception of a three-fold decreased expression of the MCM6 minichromosome maintenance deficient gene (MCM6, 25% of GAPD) at 12 h, followed at 48 h by a two-fold increased expression of the S-phase kinase-associated protein 1A (SKP1A, 29% of GAPD),

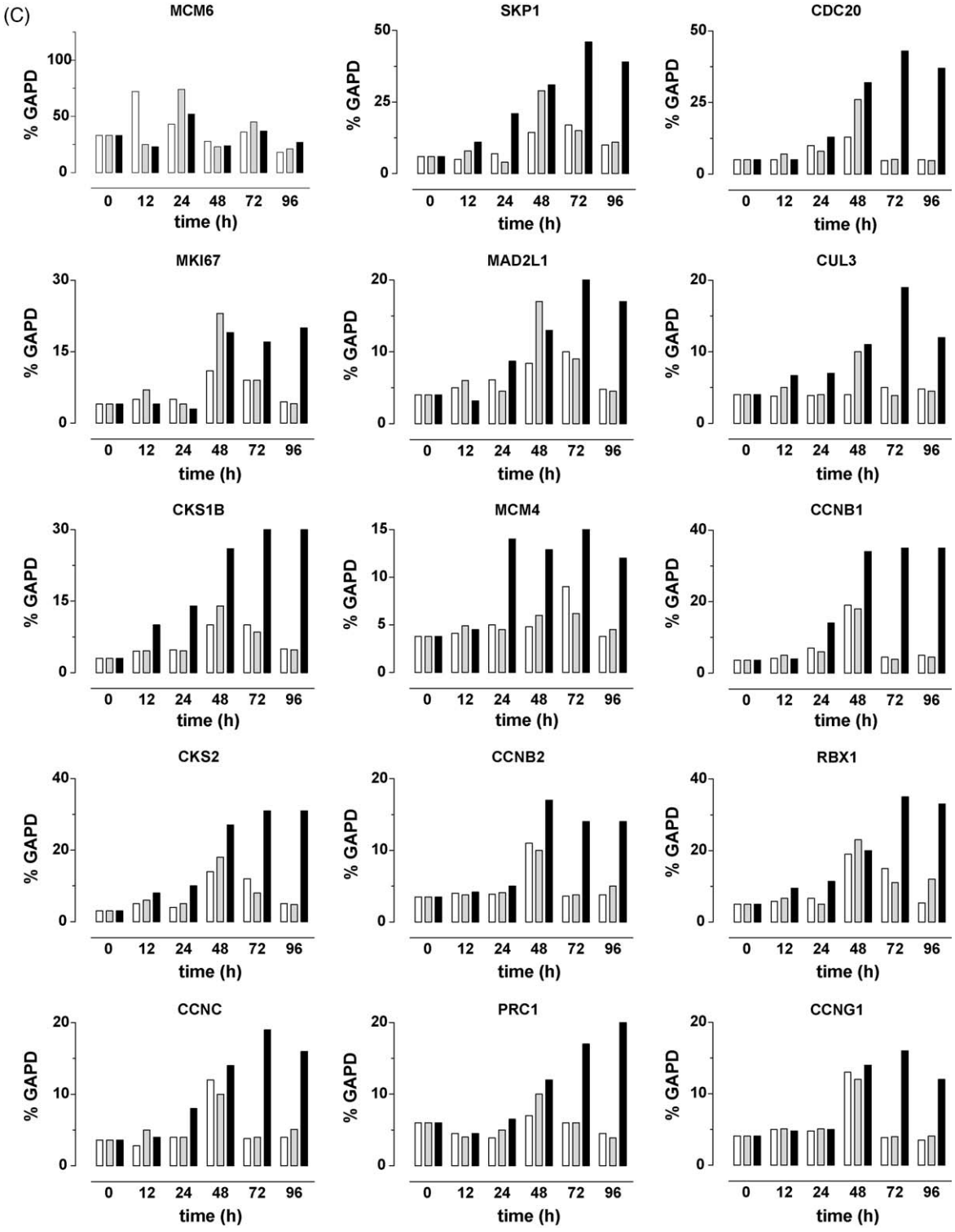

Fig. 4. (Continued).

CDC20 cell division cycle 20 homolog (CDC20, 26% of GAPD), Ki-67 antigen (MKI67, 23% of GAPD), MAD2 mitotic arrest deficient-like 1 (MAD2L1, 17% of GAPD), and Cullin 3 (CUL3, 10% of GAPD) genes.

In the case of *trans*-Z-treated SKOV-3 cells, twelve hours after the beginning of the treatment the MCM6 gene expression was three-fold decreased (MCM6, 23% of GAPD), whereas two genes were induced to levels two times higher than control, the S-phase kinase-associated protein 1A (SKP1A, 11% of GAPD), and the CDC28 protein kinase regulatory subunit 1B (CKS1B, 10% of GAPD). The up-regulation of SKP1A and CKS1B was maintained up to 96 h. Other genes became up-regulated at 24, 48, or 72 h incubation time. Two-fold up-regulated at 24 h were: MCM4 minichromosome maintenance deficient 4 (MCM4, 14% of GAPD), cyclin B1 (CCNB1, 14% of GAPD), and CDC28 protein kinase regulatory subunit 2 (CKS2, 10% of

Table 1 – Time-course of expression of selected genome stability/DNA repair, and checkpoint/cell cycle progression genes in SKOV-3 cells treated with equitoxic concentrations of *trans*-DDP or *trans*-Z[a]

Gene	Treatment	0 h	12 h	24 h	48 h	72 h	96 h
APEX1	Control	9	12.1	12	13	10	11
	trans-DDP	9	9	8	15	12	10
	trans-Z	9	11	12	14	12	10
NEIL3	Control	5	5	4.9	5.2	7	6
	trans-DDP	5	5.3	5.2	5.6	6.1	6
	trans-Z	5	6	5.1	7	7	5.1
UNG	Control	6	6	5.3	5.2	6	5.1
	trans-DDP	6	5.8	5.4	6	5.1	5.3
	trans-Z	6	5.2	5.2	6	7	5.3
G22P1	Control	26	27	35	37	27	31
	trans-DDP	26	26	31	35	30	28
	trans-Z	26	33	30	41	28	30
DDB1	Control	8	9	9	10	10	8
	trans-DDP	8	8	10	9	10	9
	trans-Z	8	8	10	11	12	8
XRCC5	Control	31	30	27	33	36	27
	trans-DDP	31	24	23	27	24	28
	trans-Z	31	25	27	36	28	30
XRCC4	Control	12.1	14	9	10	10	9
	trans-DDP	12.1	13	11	10	12	8
	trans-Z	12.1	11	9	10	11	10
UBE2V2	Control	5	5.3	5	7	5	6
	trans-DDP	5	5.1	6	8	5	7
	trans-Z	5	5.2	5.2	7	6	7
GADD45	Control	7	8	6	5.6	6.7	6
	trans-DDP	7	21	14	7	8	5.6
	trans-Z	7	24	17	13	17	20
TERF-2	Control	40	30	21	27	41	35
	trans-DDP	40	35	27	100	60	45
	trans-Z	40	32	27	96	55	52
UBE3A	Control	10	5	5.5	8	5.6	11
	trans-DDP	10	5	6	20	6	9
	trans-Z	10	13	11	22	21	15
UBE1	Control	6	9	7	5	6	4.8
	trans-DDP	6	10	8	13.5	6	5.3
	trans-Z	6	12	7	14	14.5	12
PRCDC	Control	10	7	8	9	8	12
	trans-DDP	10	6	9	10	22	10
	trans-Z	10	7	18	18	24	11
UBC	Control	28	18	35	50	66	39
	trans-DDP	28	26	30	85	49	53
	trans-Z	28	58	76	95	123	95
RAD23A	Control	9.1	6.2	10.2	9	8.4	11
	trans-DDP	10	8	9	18	10	10
	trans-Z	10	18	20	22	17	13
RAD18	Control	5.4	4.5	5.6	6.1	5	5.3
	trans-DDP	5.4	5	5.4	5.4	4	5.7
	trans-Z	5.4	11	17	11	10.2	5.9
RPA1	Control	5	4	5	4	4	4
	trans-DDP	5	5.1	4	5	5	5
	trans-Z	5	4	13	14	12	5
SUMO1	Control	11	10	5.5	4.5	6	13
	trans-DDP	11	10	6	11.5	7.5	11
	trans-Z	11	15	13	14	18	11

Table 1 (*Continued*)

Gene	Treatment	0 h	12 h	24 h	48 h	72 h	96 h
RAD50	Control	4	4.6	4.8	5.1	4.9	5.3
	trans-DDP	4	5	4.8	6	5	6
	trans-Z	4	4.8	12.6	13	11	5.5
RPA2	Control	7	4.8	5	5.4	5	5
	trans-DDP	7	5	5	5	6	6
	trans-Z	7	5	5.5	12	5.2	5.4
CHK1	Control	4	4.5	5	11	10	4.6
	trans-DDP	4	4.7	4.7	15	7	5.1
	trans-Z	4	4.7	5.8	23	30	30
UBE2A	Control	5.4	5.8	5.5	4.9	5.7	6
	trans-DDP	5.4	4.8	5.4	5.6	5.7	5.6
	trans-Z	5.4	5	5.5	12	11.4	5
MCM6	Control	33	72	43	28	36	18
	trans-DDP	33	25	74	23	45	21
	trans-Z	33	23	52	24	37	27
SKP1	Control	6	5	7	14.4	17	10
	trans-DDP	6	8	4	29	15	11
	trans-Z	6	11	21	31	46	39
CDC20	Control	5	5	10	13	4.8	5.1
	trans-DDP	5	7	8	26	5.2	4.8
	trans-Z	5	5	13	32	43	37
MKI67	Control	4	5	5	11	9	4.5
	trans-DDP	4	7	4	23	9	4.1
	trans-Z	4	4.8	5.3	19	17	20
MAD2L1	Control	4	5	6.1	8.4	10	4.8
	trans-DDP	4	6	4.5	17	9	4.5
	trans-Z	4	5.2	8.7	13	21	17
CUL3	Control	4	4.8	4.9	5.1	5	5.8
	trans-DDP	4	5	4.9	10	5.9	5.5
	trans-Z	4	6.7	7	11	19	12
CKS1B	Control	5	4.5	4.8	10	10	5
	trans-DDP	5	4.6	4.6	14	8.5	5.8
	trans-Z	5	10	14	26	30	30
MCM4	Control	5.8	5.4	5	5.8	9	4.8
	trans-DDP	5.8	4.9	5	6	6.2	5.5
	trans-Z	5.8	4.5	14	13	17	12
CCNB1	Control	4.6	5.2	7	19	5.5	5.6
	trans-DDP	4.6	5	6	18	5.4	5.5
	trans-Z	4.6	4	14	34	35	35
CKS2	Control	4.3	5	4.5	14	12	5
	trans-DDP	4.3	6	5	18	8	4.8
	trans-Z	4.3	8	10	27	31	31
CCNB2	Control	4.8	5.4	5.9	11	5.6	5.3
	trans-DDP	4.8	4.8	4.1	10	4.8	5
	trans-Z	4.8	4.2	5	17	14	14
RBX1	Control	5	5.8	6.6	19	15	5.4
	trans-DDP	5	6.7	5	23	11	12
	trans-Z	5	9.5	11.4	20	35	33
CCNC	Control	5.1	4.8	5.4	12	4.8	4.6
	trans-DDP	5.1	5	4	10	4	5.1
	trans-Z	5.1	4	8	14	19	16
PRC1	Control	6	4.5	5.9	7	6	4.5
	trans-DDP	6	4	5	10	6	4.4
	trans-Z	6	4.5	6.5	12	17	20

Table 1 (*Continued*)

Gene	Treatment	0 h	12 h	24 h	48 h	72 h	96 h
$CCNG_1$	Control	5.4	5	4.8	13	4.9	4.5
	trans-DDP	5.4	5.1	5.1	12	4	4.1
	trans-Z	5.4	4.8	5	14	16	12

[a] Exponentially growing SKOV-3 cells were exposed to IC_{50} concentrations of *trans*-DDP or *trans*-Z (170 and 120 μM, respectively) over a 96 h continuous treatment. At different time points (0, 12, 24, 48, 72, and 96 h), the expression profile of 188 genes known to be associated with maintaining genome stability/DNA repair, and regulating checkpoint/cell cycle progression was analyzed by using GEArray™ Q series cDNA expression array membranes (SuperArray Inc., Bethesda, MD, USA). After hybridization, data were acquired with a phosphor screen scanner, and analysed (pUC 18 plasmid DNA background subtraction, and normalization to GAPDH house-keeping gene). Each experiment was performed twice with similar results, the duplicate results for each gene being within 8% of the mean for that gene. The mean values of the two series are presented for the genes whose expression was at least 4% of that of GAPDH.

GAPD). Two-fold up-regulated at 48 h were: CDC20 cell division cycle 20 homolog (CDC20, 32% of GAPD), Antigen identified by monoclonal antibody Ki-67 (MKI67, 19% of GAPD), cyclin B2 (CCNB2, 17% of GAPD), and cullin 3 (CUL3, 11% of GAPD). Finally, two-/three-fold up-regulated at 72 h were: ring-box 1 (RBX1, 35% of GAPD), MAD2 mitotic arrest deficient-like 1 (MAD2L1, 21% of GAPD), cyclin C (CCNC, 19% of GAPD), Protein regulator of cytokinesis 1 (PRC1, 17% of GAPD), and cyclin G_1 ($CCNG_1$, 16% of GADP). Up-regulated genes generally maintained similar overexpression levels in the following treatment times, in some cases further increasing their overexpression with respect to control (CCNB1, CDC20, CKS2, and RBX1).

4. Discussion

In the search for new platinum drugs different from cisplatin and classical analogues there has been, in recent years, an increasing interest in *trans* platinum complexes. Among them, the DNA-damaging platinum–iminoether complex *trans*-$[PtCl_2(NH_3)\{Z\text{-}HN = C(OMe)Me\}]$ (*trans*-Z) is characterized by having: (i) spectrum of action different from that of cisplatin as well as from that of transplatin, (ii) efficacy towards cisplatin-resistant tumour cells, and (iii) in vivo activity similar to that of cisplatin towards murine tumours and human SKOV-3 xenografts [14,15]. Mechanistic investigations of *trans*-Z have shown that DNA interaction properties of this antitumour-active *trans* platinum compound are very similar to those of the antitumour-inactive *trans*-DDP [14]. However, the two compounds might be different in their ability of reaching cellular DNA, and it has been reported that iminoether ligands favour cellular accumulation of platinum compounds [8,9]. Moreover, although *trans*-Z and *trans*-DDP form the same type of adducts at the same sites on DNA, the overall three-dimensional structure of the adducts is different, and therefore could be differently recognised by cellular proteins. This study compares cellular accumulation and DNA platination of SKOV-3 ovarian cancer cells after *trans*-DDP or *trans*-Z, and focuses on cellular response to treatment. Thus growth inhibition and cell death, cell-cycle progression, and gene expression modifications of SKOV-3 cells exposed to IC_{50} concentrations of *trans*-Z or *trans*-DDP have been analyzed in parallel. Our aim was to explore the determinants of cellular response to *trans*-Z or *trans*-DDP, i.e. which cellular pathways were activated during the treatment, and which different cellular processing of drug-induced damage could contribute to explain the molecular basis of *trans*-Z antitumour activity in the SKOV-3 system.

The results of cellular accumulation and DNA platination indicate that *trans*-Z and *trans*-DDP enter cells with the same efficacy. However, *trans*-Z shows a two-fold higher affinity for cellular DNA. A possible explanation for such a difference is that the bulky iminoether group can retard ligand substitution reactions at the chloride ligands, thereby reducing undesired reactions between *trans*-Z and cellular components, and facilitating its interaction with DNA.

As to the effect of treatment upon cell growth and cell-cycle progression, *trans*-DDP determines an initial and transient cytostatic effect, paralleled by a moderate increase of apoptosis and by sequential arrests in S and G_2/M phases of the cell-cycle. In contrast, *trans*-Z determines an initial cytotoxic effect, along with a more persistent and marked increase of apoptosis and a more marked and prolonged arrest in S and G_2/M phases of the cell-cycle.

Pathway-specific gene expression modifications indicate that *trans*-DDP-treated cells transiently increase the expression of GADD45A gene, in coincidence with the cytostatic effect and the arrests in S and G_2/M phases. GADD45A transcript levels are generally increased by environmental stresses (growth arrest conditions and DNA-damaging treatments). GADD45A transcription can be stimulated by p53-dependent or -independent mechanisms, and the corresponding protein activates the p38/JNK pathway, thus playing a regulating role in cell-cycle arrest and in the balance between survival and apoptosis [20]. Interestingly, *trans*-DDP determines also an early decrease of MCM6 transcription, whose corresponding protein belongs to the MCM complex, which regulates DNA replication [21]. These early modifications are followed by the overexpression of genes involved in regulating telomere protection (TERF2), S-phase (proliferation-related Ki-67 antigen), and M-phase (CDC20 and MAD2L1)), this happening in concomitance with proliferation restart and cell-cycle arrest release. In parallel, some ubiquitin system genes (ubiquitin protein ligases UBE3A and CUL3 and ubiquitin-like SUMO-1) appear up-regulated, thus indicating that also protein degradation and post-translational modifications are involved in cellular response during *trans*-DDP treatment. Finally, there is a late up-regulation of the catalytic subunit of the DNA-dependent protein kinase (PRKDC), while the genes coding for the regulatory component Ku of the enzyme (G22P1 and XRCC5) are transcribed without modifications with respect to control.

The same genes whose expression is modified by *trans*-DDP are also modified by *trans*-Z. However, *trans*-Z determines an up-regulation more persistent in the case of GADD45A, CDC20, MKI67, CUL3, and MAD2L1, and more precocious and persistent in the case of UBE3A, SUMO-1, and PRKDC. Importantly, cellular response to *trans*-Z includes also the overexpression of a number of other genes whose function is related to DNA repair, such as RPA1, RPA2, RAD23A, and RAD50. RPA1 and RPA2 genes code for single-strand DNA binding proteins largely involved in DNA metabolism and repair [22], and RAD23A and RAD50 encode for proteins involved in the nucleotide excision repair and in the double strand break repair, respectively [23,24]. Moreover, both RAD23A and RAD50 proteins interact with other proteins that connect DNA repair and cell-cycle progression, so they have a general role in the global cellular response to DNA damage [25]. *Trans*-Z treatment also up-regulates the cell-cycle checkpoint CHK1 gene, thus indicating an involvement of the ATR/CHK1 pathway, which likely contributes to the observed G_2/M block [26]. A number of other genes whose products control cell-cycle progression are also induced by *trans*-Z. Interestingly, their up-regulation coincides with proliferation restarting and endures throughout the subsequent normalization of cell-cycle distribution. Among them, cyclins B1, B2, C, and G_1, cyclin-dependent kinase regulatory subunits CKS1 and CKS2, replication protein MCM4, cytokinesis protein PRC1, as well as ubiquitin genes with functions related to DNA repair (RAD18, UBE2A) and cell-cycle progression (UBC, UBE1, SKP1, RBX).

An overall analysis of the pathway-specific gene expression modifications induced by treatment indicates that phenotypic effects of *trans*-DDP are driven by an initial and transient up-regulation of some genes related to cell-cycle checkpoint and arrest networks. In contrast, the more dramatic phenotypic effects of *trans*-Z are driven by a persistent up-regulation of more numerous genes, involved in cell-cycle checkpoint and arrest networks, and in genome stability and DNA repair. Therefore, molecular and cellular events have been identified which are produced by *trans*-Z but not by *trans*-DDP, and which likely represent the mechanistic basis of the antitumour activity of *trans*-Z in the SKOV-3 system.

Since DNA represents the pharmacological target of both *trans*-DDP and *trans*-Z, and cellular DNA platination levels are quite similar after 3-h exposure to IC_{50} concentrations, it can be hypothesized that the different cellular response to *trans*-DDP and *trans*-Z depends upon a different persistence of Pt–DNA adducts, longer for *trans*-Z than for *trans*-DDP. This in turn could be due to a more prolonged cellular entrance of *trans*-Z as well as to intrinsic features of the *trans*-Z-DNA monofunctional adducts [14]. While further measurements of cellular DNA platination and Pt–DNA adduct removal are needed for a definite evidence of the above hypothesis, it can be speculated that the major kinetic stability of *trans*-Z could prolong cell penetration with respect to *trans*-DDP, which no longer enters cells after 3 h incubation, as a consequence of reaction with the culture medium [27]. On the other hand, DNA monofunctional adducts of *trans*-Z are more stable than the corresponding adducts of *trans*-DDP [14], and the formation of persistent monofunctional adducts appears to be a common feature of platinum complexes with iminoethers [6]. Interestingly, DNA monofunctional adducts of the parent complex *trans*-[$PtCl_2$(E-iminoether)$_2$] have been recently shown to form easily DNA–protein ternary complexes [28], thus further indicating that intrinsic features of Pt–iminoether monofunctional adducts can play a central mechanistic role.

In conclusion, the results indicate that SKOV-3 cellular pathways activated by the antitumour-active *trans*-Z are different from those activated by *trans*-DDP. Importantly, the pathway-specific gene expression modifications analysed by microarrays are validated in the present work by the correlations with the parallel biological assays of cellular proliferation, cell cycle perturbation, and apoptosis. This initial knowledge of the damage processing provides an important basis for more detailed functional investigations of genes modified by *trans*-Z (RT-PCR, RNAi). In a near future, we can reasonably expect to be able of defining the whole picture of genes, gene products, and pathways that drive pharmacological response of tumour cells to *trans*-Z, thus laying the basis for the comprehension of the therapeutic potential and for the rational design of antitumour *trans* platinum compounds.

Acknowledgements

We are grateful to A. De Cataldo, N. Cardellicchio, and M. Sivo for atomic absorption measurements, and to F. Intini for providing the *trans*-[$PtCl_2(NH_3)${Z-HN = C(OMe)Me}] (*trans*-Z) complex. The work has been supported by grants from Regione Puglia (Ricerca finalizzata 2002–2003 DL229/99), MIUR (PRIN 2004059078), and EU (COST D20/0003/01).

REFERENCES

[1] O'Dwyer P, Stevenson J, Johnson S. Clinical pharmacokinetics and administration of established platinum drugs. Drugs 2000;59:19–27.
[2] Xin Zhang C, Lippard SJ. New metal complexes as potential therapeutics. Curr Opin Chem Biol 2003;7:481–9.
[3] Natile G, Coluccia M. Current status of *trans*-platinum compounds in cancer therapy. Coord Chem Rev 2001;216/217:383–410.
[4] Coluccia M, Nassi A, Loseto F, Boccarelli A, Mariggiò MA, Giordano D, et al. A *trans* platinum complex showing higher antitumor activity than the *cis* congeners. J Med Chem 1993;36:510–3.
[5] Coluccia M, Boccarelli A, Mariggiò MA, Cardellicchio N, Caputo P, Intini FP, et al. Platinum(II) complexes containing imino ethers: a *trans* platinum antitumor agent. Chem–Biol Interact 1995;98:251–66.
[6] Natile G, Coluccia M. Antitumor-active *trans*-platinum compounds. Met Ions Biol Syst 2004;42:209–50.
[7] Boccarelli A, Coluccia M, Intini FP, Natile G, Locker D, Leng M. Cytotoxicity and DNA binding mode of new platinum iminoether derivatives with different configuration at the iminoether ligands. Anti-cancer Drug Des 1999;14:253–64.
[8] Coluccia M, Nassi A, Boccarelli A, Giordano D, Cardellicchio N, Locker D, et al. In vitro and in vivo antitumor activity and cellular pharmacological properties of new platinum imninoether complexes with different configuration at the iminoether ligands. J Inorg Biochem 1999;77:31–5.

[9] Coluccia M, Nassi A, Boccarelli A, Giordano D, Intini FP, Natile G, et al. In vitro antitumour activity and cellular pharmacological properties of the platinum iminoether complex *trans*-[$PtCl_2${E-HN = C(OMe)Me}$_2$]. Int J Oncol 1999;15:1039–44.
[10] Janovska E, Novakova O, Natile G, Brabec V. Differential genotoxic effects of antitumour *trans*-[$PtCl_2$(E-iminoether)$_2$] and cisplatin in *Escherichia coli*. J Inorg Biochem 2002;90: 155–8.
[11] Brabec V, Vrana O, Novakova O, Kleinwachter V, Intini FP, Coluccia M, et al. DNA adducts of antitumour *trans*-[$PtCl_2$(E-imino ether)$_2$]. Nucl Acids Res 1996;24:336–41.
[12] Ialudova R, Iakovska A, Parkova I, Balkarova Z, Vrana O, Coluccia M, et al. DNA modifications by antitumour *trans*-[$PtCl_2$(E-iminoether)$_2$]. Mol Pharmacol 1997;52:354–61.
[13] Andersen B, Margiotta N, Coluccia M, Natile G, Sletten E. Antitumour *trans* platinum-DNA adducts: NMR and HPLC study of the interaction between a *trans*-Pt(iminoether) complex and the deoxy decamer d(CCTCGCTCTC) d(GAGAGCGAGG). Metal-based Drugs 2000;7:23–32.
[14] Leng M, Locker D, Giraud-Panis MJ, Schwartz A, Intini FP, Natile G, et al. Replacement of a NH_3 by an iminoether in transplatin makes an antitumour drug from an inactive compound. Mol Pharmacol 2000;58:1525–35.
[15] Intini FP, Boccarelli A, Francia V, Natile G, Giordano D, De Rinaldis P, et al. Platinum complexes with iminoethers or cyclic ligands mimicking iminoethers; synthesis, antitumour activity and DNA interaction properties. J Biol Inorg Chem 2004;9:768–80.
[16] Brabec V, Sip M, Leng M. DNA conformational change produced by the site-specific interstrand cross-link of *trans*-diamminedichloroplatinum(II). Biochemistry 1993;32:11676–81.
[17] Sambrook J, Fritsch E, Maniatis T. Molecular cloning: a laboratory manual New York: Cold Spring Harbor Laboratory Press; 1989.
[18] Burton K. A study of the conditions and mechanism of the diphenylamine reaction for the colorimetric estimation of deoxyribonucleic acid. Biochem J 1956;62:315–23.
[19] Gong J, Traganos F, Darzynkiewicz Z. A selective procedure for DNA extraction from apoptotic cells applicable for gel electrophoresis and flow cytometry. Anal Biochem 1994;218:314–9.
[20] Zhan Q. Gadd45a, a p53- and BRCA1-regulated stress protein, in cellular response to DNA damage. Mutat Res 2005;1/2:133–43.
[21] Johnson EM, Kinoshita Y, Daniel DC. A new member of the MCM protein family encoded by the human MCM8 gene, located contrapodal to GCD10 at chromosome band 20p12 3–13. Nucl Acids Res 2003;11:2915–25.
[22] Binz SK, Sheehan AM, Wold MS. Replication protein A phosphorylation and the cellular response to DNA damage. DNA Rep 2004;8–9:1015–24.
[23] Sugasawa K, Ng JM, Masutani C, Iwai S, van der Spek PJ, Eker AP, et al. Xeroderma pigmentosum group C protein complex is the initiator of global genome nucleotide excision repair. Mol Cell 1998;2:223–32.
[24] Huang J, Dynan WS. Reconstitution of the mammalian DNA double-strand break end-joining reaction reveals a requirement for an Mre11/Rad50/NBS1-containing fraction. Nucl Acids Res 2002;3: 667–74.
[25] Robison JG, Lu L, Dixon K, Bissler JJ. DNA lesion-specific co-localization of the Mre11/Rad50/Nbs1 (MRN) complex and replication protein A (RPA) to repair foci. Biol Chem 2005;13:12927–34.
[26] Bartek J, Lukas J. Chk1 and Chk2 kinases in checkpoint control and cancer. Cancer Cell 2003;3:421–9.
[27] Johnson NP, Lapetoule P, Razaka H, Villani G. Biological and biochemical effects of DNA damage caused by platinum compounds. In: McBrien DHC, Slater TF, editors. Biochemical mechanisms of platinum antitumour drugs. Oxford: IRL Press Ltd.; 1985. p. 1:20.
[28] Novakova O, Kasparkova J, Malina J, Natile G, Brabec V. DNA-protein cross-linking by *trans*-[PtCl(2)(E-iminoether)(2)]. A concept for activation of the *trans* geometry in platinum antitumour complexes. Nucl Acids Res 2003;31:6450–60.